

SUPPORTING MATERIAL

**Crystal structures of the L<sub>1</sub>, L<sub>2</sub>, N, and O states of *pharaonis* halorhodopsin**

**Tsutomu Kouyama<sup>1,2</sup>, Haruki Kawaguchi<sup>1</sup>, Taichi Nakanishi<sup>1</sup>, Hiroki Kubo, ,  
and Midori Murakami<sup>1</sup>**

<sup>1</sup>Department of Physics, Graduate School of Science, Nagoya University, Furo-cho, Chikusa-ku, Nagoya, Japan. <sup>2</sup>RIKEN Harima Branch, 1-1-1, Kouto, Sayo, Hyogo, Japan

Correspondence should be addressed to T. K. (kouyama@bio.phys.nagoya-u.ac.jp)

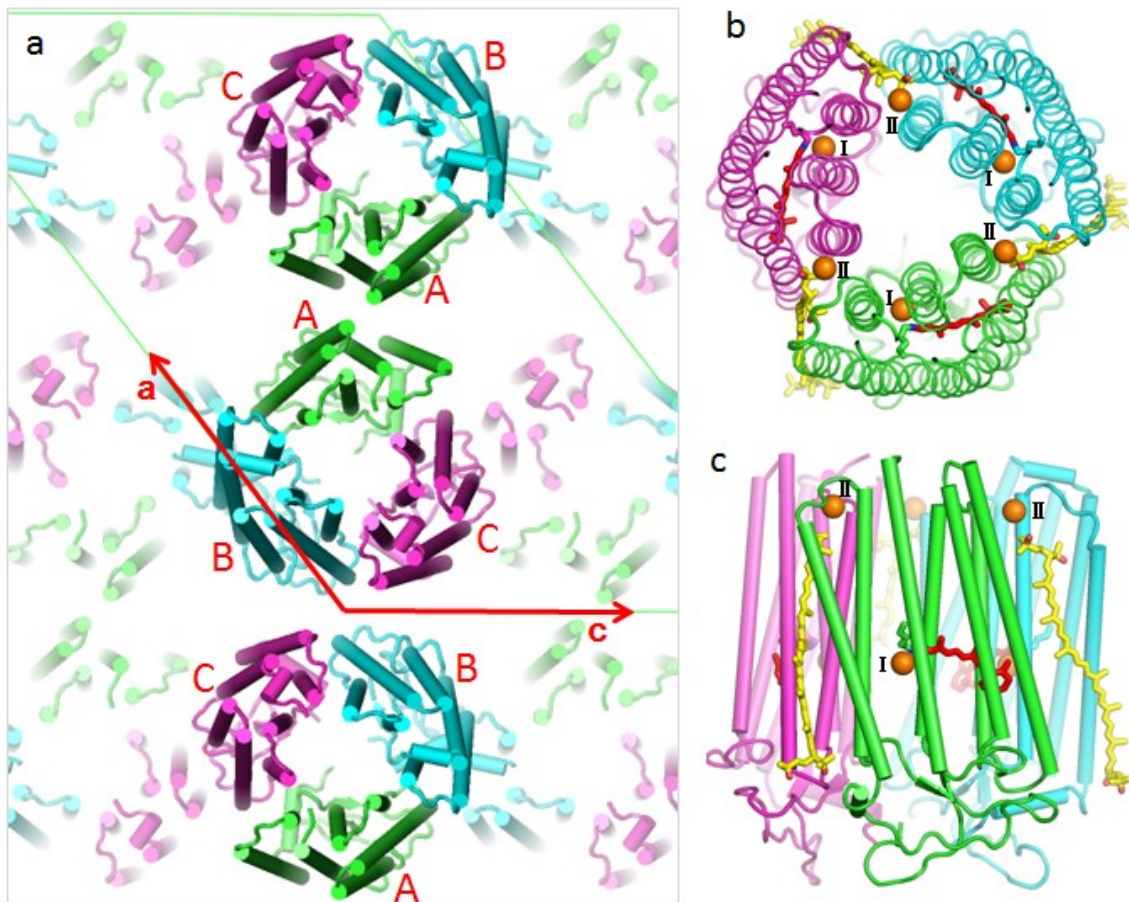


**Figure S1.** The crystal packing in the C2 crystal of pHR and the structure of the trimeric pHR-bacterioruberin complex in the resting state. **a)** The arrangement of the pHR trimers in the C2 crystal is viewed along the *b*-axis. **b)** and **c)** Top and side views of the pHR trimer. The orange spheres represent the halide ions bound to site I and II. Bacterioruberin molecules bound to the inter-subunit crevices are shown by yellow sticks.

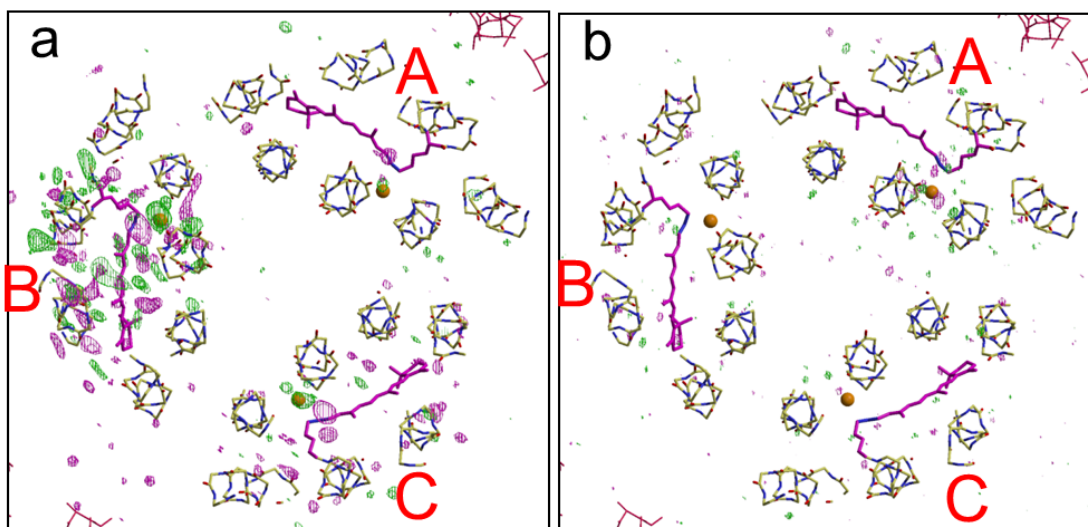


**Figure S2. Light-induced structural changes vs. X-ray-induced structural changes.** **a)** The diffraction amplitudes ( $|F_{\text{light}}|$ ) from a crystal that had been soaked in 1.5 M Na-citrate and 0.1 M NaBr., illuminated at 240 K and cooled to 100 K was compared with those ( $|F_{\text{dark}}|$ ) observed for an un-illuminated crystal. The  $|F_{\text{light}}| - |F_{\text{dark}}|$  difference map is contoured at  $3.4 \sigma$  (positive, purple; green, negative) and overlaid on the structural model of the resting state. The orange spheres represent the bromide ions bound to site I. **b)** The full diffraction dataset (180 images) from the illuminated crystal (used in panel a) was divided into two parts, and the diffraction amplitudes ( $F_{1\text{st}}$ ) derived by merging the first 120 images was compared with those ( $F_{2\text{nd}}$ ) derived from the last 110 images. The  $|F_{1\text{st}}| - |F_{2\text{nd}}|$  difference map is contoured at the same level as used in panel a. For collection of the full dataset, the crystal was exposed to an X-ray flux of  $\sim 1 \times 10^{15}$  photons/mm<sup>2</sup>. At this low X-ray flux, no significant X-ray-induced structural change was detected.

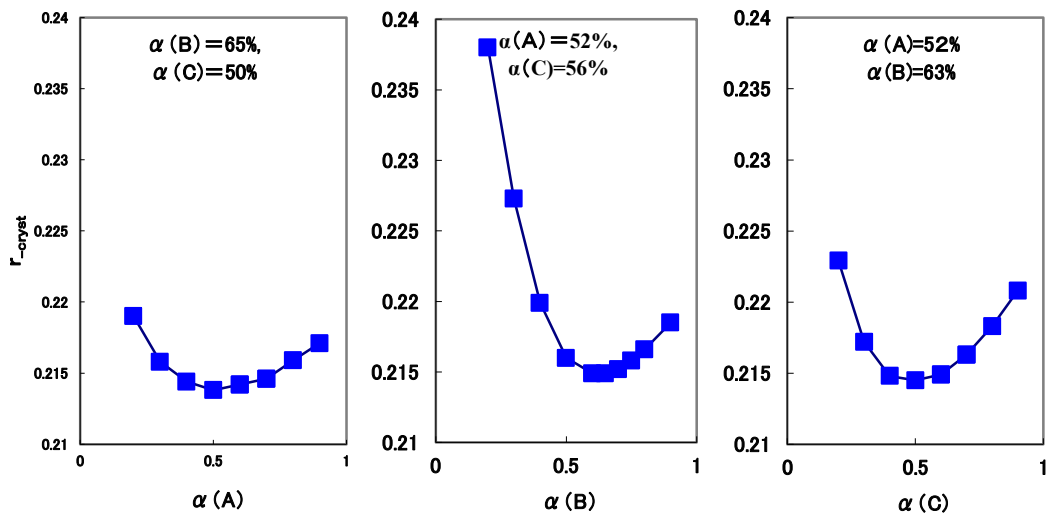


**Figure S3. Estimation of the occupancy  $\alpha_i$  of a reaction state trapped in the  $i$ -th subunit within the asymmetric unit of the C2 crystal.** Estimation of the occupancy  $\alpha_i$  of a reaction state trapped in the  $i$ -th subunit (subunit A, B or C) within the asymmetric unit of the C2 crystal of the pHR-bromide complex that was soaked in a post-crystallization solution consisting of 0.1 M NaBr, 1.5 M Na-citrate, 0.1 M HEPES at pH 7 and 30% trehalose, illuminated at 240 K with orange light for 1 min, and cooled to 100 K with a cooling rate of 2.3 K/sec. Under these illumination conditions, the N state was preferentially trapped in subunit B. The structural analysis was performed on the approximation that each subunit contains two conformers (a reaction state and the resting state). In each panel, the  $R_{\text{cryst}}$  value ( $= \sum_{\text{hkl}} (|F_{\text{obs}}| - |F_{\text{calc}}|) / \sum_{\text{hkl}} |F_{\text{obs}}|$ ) is plotted as a function of the occupancy  $\alpha_i$  ( $i=1, 2, 3$ ); each curve was evaluated using the optimal  $\alpha_j$  ( $j \neq i$ ) values of the reaction states in the other subunits.

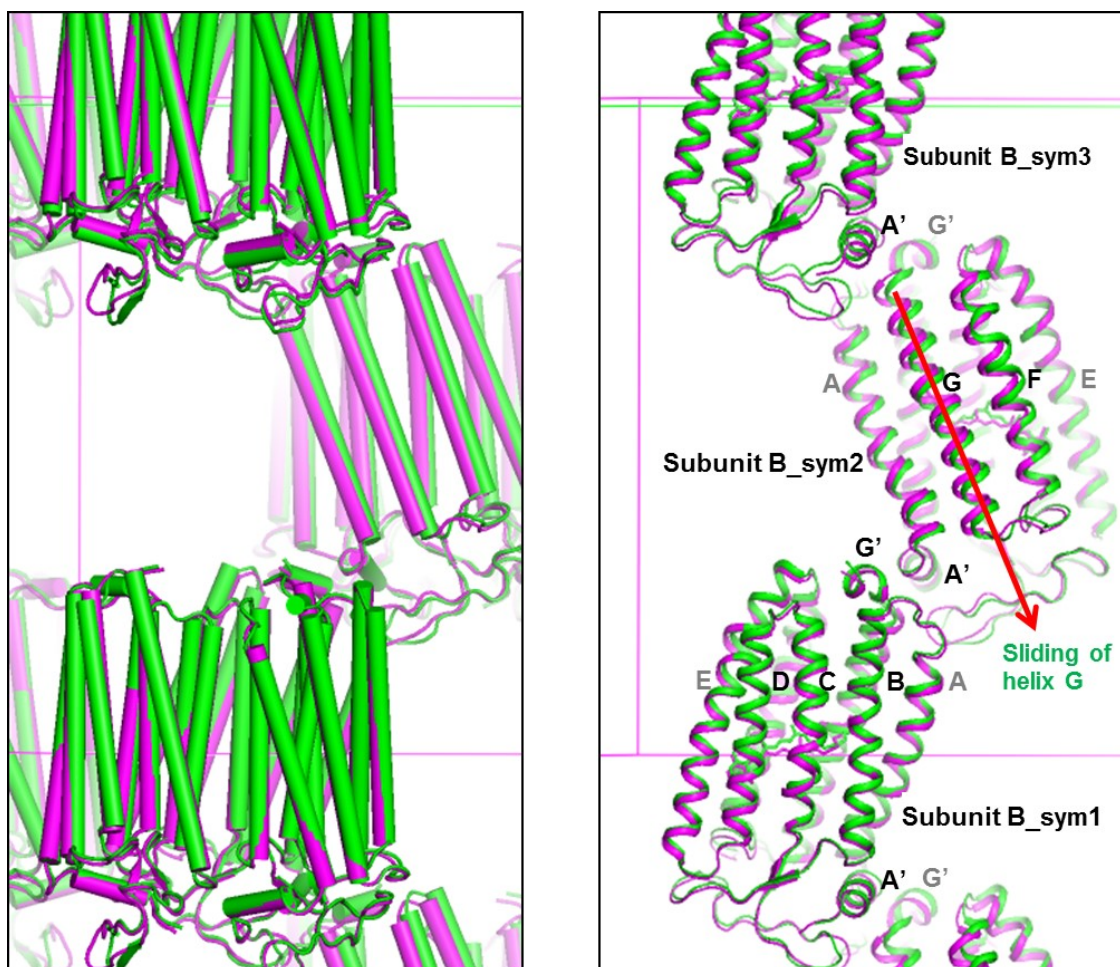


**Figure S4. Light-induced shrinkage of the unit cell at 240 K.** a) Notable shrinkage of the unit cell along the b axis was observed when a large amount of the N state accumulated under illumination at 240 K. In the figure, the structure of the N state (green) in the illuminated crystal is compared with that of the resting state (magenta) in an un-illuminated crystal. The N state shown here was trapped in subunit B when the crystal that had been soaked in a solution containing 0.1 M bromide ions was cooled to 100 K with a cooling rate of 2.3 K/sec after illumination at 240 K. b) For clarity, only proteins (subunit B) around a two-fold screw axis are shown; the other subunits contained in the asymmetric unit are omitted. Owing to the protein-protein contact between neighboring proteins (subunit B) related by a two-fold screw axis, the motional freedom of helix G in subunit B is very restricted. On the other hand, the EF loop in subunit B faces an open space so that the residues in the extracellular half of helices E and F have a relatively larger B factor as compared to the corresponding residues in subunit A.

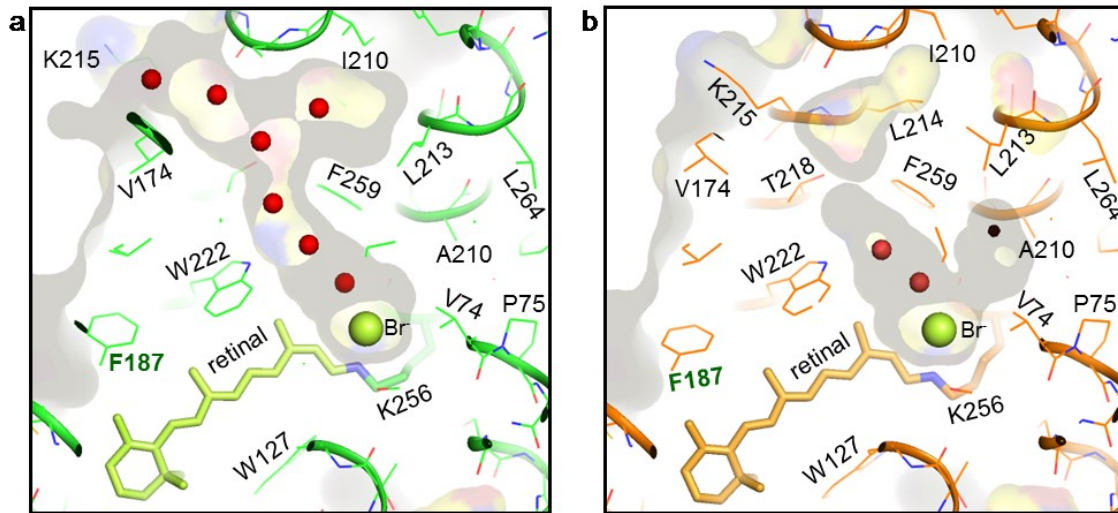


**Figure S5. Morphological changes in the internal cavities upon the formation of the N state in subunits B and an N-like state in subunit C.** a) A long cavity extending from the Schiff base to the cytoplasmic surface is created in the N state that was trapped in subunit B when the crystal that had been soaked in a solution containing 0.1 M bromide ions was cooled to 100 K with a cooling rate of 2.3 K/sec after illumination at 240 K. b) A reaction state with a bromide ion at site *i*134 was trapped in subunit C within the same crystal. This reaction state resembles the N state trapped in subunit B, but the opening of the anion-release pathway is incomplete in subunit C. A smaller light-induced outward movement of helix F in subunit C is due to inherent constraints by the crystal lattice force; note that the EF loop of subunit C is involved in protein-protein interactions between adjacent proteins related by a two-fold screw axis.

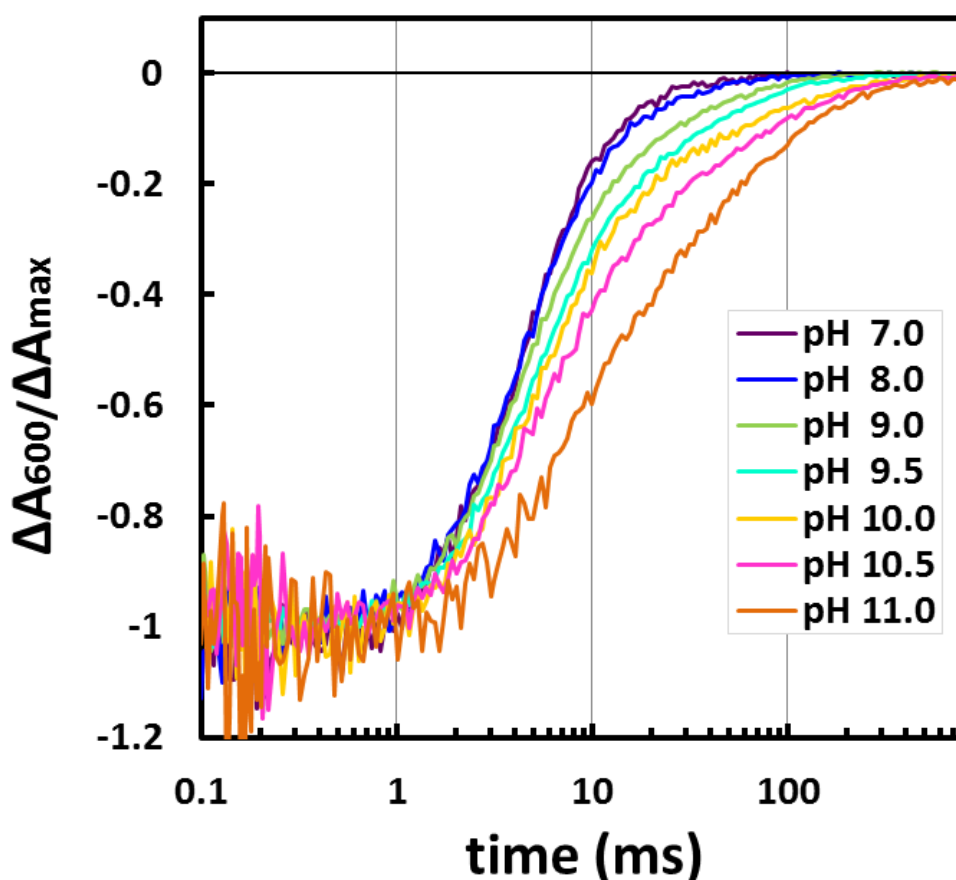


**Figure S6. pH dependence of the rate of the N-to-O transition.** Light-induced absorption changes at 600 nm in a suspension of claret membrane at 293 K were measured at various pH levels in the presence of 4 M NaBr and 0.1 M glycine. From the analysis of light-induced absorption changes observed at various bromide ion concentrations, it was shown that the difference absorption spectrum associated with the N-to-O transition has a broad positive peak at 620 nm and a negative peak at 520 nm, whereas the difference spectrum associated with the decay of O into the resting state has a positive peak at 570 nm and a negative peak at 640 nm. Since the absorbance of O at 600 nm is similar to that of the resting state, the absorption change at this wavelength observed in the millisecond time region is attributable to the N-to-O transition. It was therefore suggested that the N-to-O transition became slower as the medium pH was increased above pH 9. It was also suggested that in the presence of 4 M NaBr, the decay rate of O ( $k = 0.62 \pm 0.1 \text{ ms}^{-1}$ ) was higher than its formation rate and independent of the medium pH

<b>Crystal ID</b>	D-8	D-3	L-1107	L-974	L-902	L-6
Soaking solution <sup>§</sup>						
NaBr	0.1 M	0.01 M	0.01 M	0.1 M	0.01 M	0.01 M
(NH <sub>4</sub> ) <sub>2</sub> SO <sub>4</sub>	3.0 M	3.0 M	-	-	1.8 M	3.0 M
Na-citrate (pH 7)	-	-	1.5 M	1.5 M	1.0 M	-
Illumination *	Off	Off	On	On	On	On
Cooling rate	Rapid**	Rapid	Rapid	Slow-1***	Rapid	Slow-2****
Temperature	293 K → 83 K	293 K → 83 K	240 K → 83 K	240 K → 100 K	240 K → 83 K	240 K → 100 K
<b>Data collection</b>						
Space group	C2	C2	C2	C2	C2	C2
Cell dimensions						
<i>a</i> (Å)	151.93	151.62	152.77	153.37	150.74	152.22
<i>b</i> (Å)	99.48	99.50	97.95	98.30	99.45	97.57
<i>c</i> (Å)	99.60	99.53	99.77	100.53	98.55	99.72
$\beta$ (°)	127.80	127.67	128.18	128.13	127.16	128.17
Resolution (Å)	47.6-2.2	49.8-2.1	49.8-2.3	49.2-2.2	49.8-2.7	49.8-2.7
	(2.32-2.2)#	(2.21-2.1)	(2.42-2.3)	(2.32-2.2)	(2.85-2.7)	(2.85-2.7)
<i>R</i> <sub>merge</sub> (%)	11.2 (45.7)	6.8(50.7)	8.0 (49.7)	9.8(49.3)	6.0(49.1)	9.8(39.3)
<i>I</i> / $\sigma$ <i>I</i>	9.3 (3.3)	11.2(2.5)	12.0(2.7)	9.2(2.7)	10.9(2.3)	13.8(2.8)
Completeness (%)	98.7 (98.2)	99.7(99.7)	97.8(97.2)	99.0(98.5)	85.6(82.8)	96.7(86.3)
Redundancy	3.8 (3.8)	3.5(3.6)	3.1(3.2)	3.1(3.2)	10.9(2.9)	6.2(5.8)
<b>Refinement</b>						
Resolution (Å)	15.0-2.2	15.0-2.1	15.0-2.3	15.0-2.2	15.0-2.7	15.0-2.7
No. reflections	58349	58571	49977	58744	27096	
<i>R</i> <sub>work</sub> / <i>R</i> <sub>free</sub>	25.4 / 28.1	24.5 / 26.7	21.5/24.7	21.4 / 24.1	22.9 / 29.9	
No. atoms						
Protein residues	17-276	17-277	17-277	17-277	18-278	
Lipids	3	3	22	22	3	
Water	147	147	147	147	0	
Ions	6	6	5/6	5/6	3/3	
Rmsd						
Bond length (Å)	0.0071	0.0070	0.0073	0.0067	0.0077	
Bond angle (°)	1.18	1.14	1.22	1.22	1.24	
B factor (Å <sup>2</sup> )						
Protein	35.0	38.5	32.7	26.1	50.2	
Water	43.1	51.8	32.8	28.7	47.7	
Lipids / ions	90.9 / 39.7	99.2 / 55.8	75.0/44.5	64.2/44.0	- /64.8	

**Table S1. Data collection and refinement statistics.** <sup>§</sup> Other solutes: 0.04 M HEPES (pH 7) and 35 % trehalose. \* Red light ( $\lambda = 635$  nm,  $\sim 1$  mW/mm<sup>2</sup>) from a cw laser. \*\* The crystal was illuminated at 240 K and flash-cooled to 83 K with liquid propane at its melting temperature. \*\*\* The crystal was cooled in red light at a cooling rate of 2.3 K/s with temperature-controlled nitrogen gas. \*\*\*\* The crystal was cooled in the dark at a cooling rate of 2.3 K/s after illumination at 240 K with red light for  $\sim 2$  minutes. # Values in parentheses are for the highest resolution shell.